Published in final edited form as:
Bioorg Med Chem. 2012 July 15; 20(14): 4443–4450. doi:10.1016/j.bmc.2012.05.026.

Self-calibrating viscosity probes: Design and subcellular localization

Marianna Dakanali[a,*], **Thai H. Do**[a], **Austin Horn**[b], **Akaraphon Chongchivivat**[a], **Tuptim Jarusreni**[a], **Darcy Lichlyter**[b], **Gianni Guizzunti**[c], **Mark A. Haidekker**[b,*], and **Emmanuel A. Theodorakis**[a,*]

[a]Department of Chemistry & Biochemistry, University of California, San Diego, 9500 Gilman Drive MC: 0358, La Jolla, CA 92093-0358, USA

[b]Faculty of Engineering, University of Georgia, Athens, GA 30602, USA

[c]Department of Cell Biology and Infection, Membrane Traffic and Pathogenesis Unit, Pasteur Institute, Paris, France

Abstract

We describe the design, synthesis and fluorescence profiles of new self-calibrating viscosity dyes in which a coumarin (reference fluorophore) has been covalently linked with a molecular rotor (viscosity sensor). Characterization of their fluorescence properties was made with separate excitation of the units and through Resonance Energy Transfer from the reference to the sensor dye. We have modified the linker and the substitution of the rotor in order to change the hydrophilicity of these probes thereby altering their subcellular localization. For instance, hydrophilic dye **12** shows a homogeneous distribution inside the cell and represents a suitable probe for viscosity measurements in the cytoplasm. 2012 Elsevier Ltd. All rights reserved.

Keywords

Fluorescence; Ratiometric dye; Molecular rotor; Subcellular viscosity

1. Introduction

The cell biomechanics are primarily determined by the cytoskeleton, the cell membrane and the cytoplasm among which the latter two possess viscoelastic properties that change in various states of diseases. It is well documented that changes in cell membrane viscosity can affect the activity of membrane-bound proteins,[1] which in turn can lead to disorders both at the cellular[2] and organismal level.[3] For instance, cardiovascular diseases,[4] cell malignancy,[5] Alzheimer's disease,[6] diabetes,[7] hypertension[8] and aging[9] are some examples of disorders associated with changes in cell membrane viscosity. On the other hand, the effects of variations in cytoplasmic viscosity have not been widely investigated, perhaps due to the relatively difficult measurement methods available. Magnetic microparticles have been used

*Corresponding author. Tel.: +1-858-822-0456; fax: +1-858-822-0386; etheodor@ucsd.edu.

Supplementary Material
^{1}H and ^{13}C NMR spectra for all compounds.

to measure cytoplasmic viscosity;[10] however, this method demands the use of very expensive equipment, has limited temporal resolution and suffers from interactions between particles and cellular environment.[10a]

General methods for measuring bulk viscosity are the cone-and-plate viscometers and the capillary viscometers,[11] but their use is limited due to the large sample size needed and the low temporal resolution.[11b] Viscosity in microenvironments, such as in cells, can be measured with the use of fluorescence-based methods.[12,13] In addition, techniques such as fluorescence anisotropy (FA)[14] and fluorescence recovery after photobleaching (FRAP)[15] are commonly used in biological systems. Although different from each other, they both rely on the diffusivity of specific fluorophores in order to report information about the viscosity of the environment. FA shows better spatial and temporal resolution than FRAP, yet local viscosity can only approximately be computed and even minor misalignments of the polarizers can cause major measurement errors during FA-based studies.[16]

Recently, efforts have been focused on the use of environment-sensitive fluorescent probes for measuring viscosity.[13,16–17] Extended discussion and examples on fluorophores are presented in several recent reviews.[17] These probes, referred to as *molecular rotors*, form twisted intermolecular charge transfer (TICT) complexes in the excited state producing a fluorescence quantum yield that is dependent of the surrounding environment.[18] Common to their chemical structure is a motif composed of an electron donor group in π-conjugation with an electron acceptor. Upon photoexcitation, these probes can relax via two competing pathways that include: (a) fluorescence emission; or (b) mechanical non-radiative deexcitation that proceeds via bond rotations between the donor and the acceptor. Viscous environments delay the mechanical deexcitation resulting in the increase of fluorescence emission. On the other hand, in media of low viscosity, the relaxation occurs primarily through mechanical motion. Modifications in any of the individual components of molecular rotors, namely the donor, the acceptor or the π-conjugation system, can affect their fluorescence profile.[19]

The Förster-Hoffmann equation[20] describes a power law relationship between the quantum yield Φ_F of a single emission molecular rotor and the solvent viscosity (η), equation (1), where C is a dye-dependent constant and x is a constant related to dye-solvent interactions:[18a],

$$\Phi_F = C \cdot \eta^x \quad (1)$$

The emission intensity of the rotor (I_{EM}) is proportionally related to the quantum yield (Φ_F), the excitation intensity (I_{EX}), the dye concentration (c) and instrument gain factors (G).

$$I_{EM} = (G \cdot c \cdot I_{EX})\Phi_F \quad (2)$$

These above equations illustrate the drawbacks in the use of molecular rotors for viscosity studies; namely this method is sensitive to changes of the fluid optical properties and to the dye concentration. These drawbacks can be overcome by the use of a dual dye, composed of an internal reference dye bound to a molecular rotor. In this case, a second, viscosity-independent emission I_{REF} becomes available that is proportional to the same factors apart from the reference quantum yield Φ_{REF}, which is viscosity independent. The ratio of the rotor and reference emissions serves as the internal calibration emission and can be simplified to equation (3):

$$\frac{I_{EM}}{I_{REF}} = \frac{(G \cdot c \cdot I_{EX}) \cdot \Phi_F}{(G \cdot c \cdot I_{EX}) \cdot \Phi_{REF}} = \frac{C}{\Phi_{REF}} \eta^{\chi} \quad (3)$$

We have explored the above principle for the design of self-calibrating dyes.[21] Here we expand this design to the synthesis and study of self-calibrating dyes with different solubility profiles for potential applications in cell imaging. We envisioned that, by virtue of their solubility profiles, these new compounds could be localized in different parts of cells allowing studies either in the cytoplasm (hydrophilic dye) or the cell membrane (hydrophobic dye). In a similar fashion, those dyes could be used in aqueous solutions and oils, respectively, for bulk viscosity measurements.

2. Results and Discussion

2.1. Design criteria of a ratiometric self-calibrating dye

According to the general design of ratiometric dyes, illustrated in Figure 1, two fluorophores, one acting as an internal reference and the other being a molecular rotor should be covalently linked. These two fluorophores should form a resonance energy transfer (RET) pair which requires that: (a) the emission spectrum of the primary fluorophore should have a significant overlap with the excitation spectrum of the secondary fluorophore and (b) that the two fluorophores are kept within a distance approximately equal to the Förster radius.[12,22] As implied by equations (1)–(3), the primary fluorophore should be a viscosity insensitive dye (reference dye) with a high but constant fluorescence emission quantum yield and should sufficiently excite the molecular rotor (viscosity sensitive dye). Following excitation of the reference dye, the ratio of the emission A to emission B would then produce a concentration-independent self-calibrating measurement of the solvent viscosity. The structure of compound **1** highlights this design, in which a coumarin donor (primary, viscosity insensitive fluorophore) is covalently attached to an amino thiophene rotor (secondary, viscosity sensitive fluorophore) via a polymethylene linker.

For the design of more hydrophilic ratiometric dyes we chose to substitute the polymethylene linker with a triethylene glycol moiety. The 7-methoxycoumarin-3-carboxylic acid was used as the primary fluorophore and was covalently attached to either a thiophene- or an aniline-based molecular rotor. For the more lipophilic ratiometric dye, we attached the same coumarin donor to an amino-thiophene rotor via a polymethylene linker of five carbons.[21c,23] To further increase the overall lipophilicity we substituted the piperidine motif of the rotor with a more fatty dihexylamine subunit.

2.2. Synthesis of the hydrophilic linker

The synthesis of the hydrophilic linker **7** is illustrated in Scheme 1. Commercially available 2-[2-(2-chloro-ethoxy)ethoxy]ethanol (**2**) was converted to azide **3** upon treatment with sodium azide in DMF.[24] Reduction of **3** using Pd/C as catalyst formed amine **4**,[25] which was subsequently protected to yield **5**[26] in 85% yield after two steps. Esterification of alcohol **5** with cyanoacetic acid (**6**) produced the hydrophilic linker **7** in 78% overall yield.

2.3. Synthesis of ratiometric dyes

The synthesis of the hydrophilic ratiometric dye containing a thiophene-based rotor is highlighted in Scheme 2. Knövenagel condensation of **8**[27] with β-cyanoester **7** gave compound **9** in good yield as a single stereoisomer (E).[19] Deprotection of the primary amine **9** by treatment with trifluoroacetic acid, followed by coupling with *N*-succinimidyl-7-methoxycoumarin-3-carboxylate (**11**), yielded ratiometric dye **12** in 83% yield.

In a similar manner, the ratiometric dye **16** was synthesized, as depicted in Scheme 3. Knövenagel condensation of the commercially available *N,N*-dimethylamino benzaldehyde (**13**) with **7** gave rise to carbamate **14** as the E isomer.[19] Deprotection of the primary amine of **14** and coupling with **11** produced the aniline containing dye **16** in 81% yield.

The synthesis of the more lipophilic dye **24** containing the long alkyl amine substituents is highlighted in Scheme 4. Commercially available aldehyde **17** was converted to the dihexylamine derivative **18** in 83% yield.[28] Knövenagel condensation of **18** with β-cyanoester **21**[21c] gave compound **22** in very good yield as a single stereoisomer.[19] Deprotection of the primary amine **22** by treatment with trifluoroacetic acid, followed by coupling with *N*-succinimidyl-7-methoxycoumarin-3-carboxylate (**11**), yielded dye **24** in 84% yield.

2.4. Fluorescence properties of ratiometric dyes

The fluorescence viscosity studies were performed from 4.15 to 414.41 mPa•sec. The emission spectra of dyes **12**, **16** and **24** recorded either via RET or direct excitation of the rotor are presented in Figure 2. As expected, all compounds exhibited dual emission.[21c] The fluorescence spectra of the dyes when excited via RET are depicted in Figures 2a, 2d and 2g; the peaks with emission maxima at around 400 nm and 490 nm correspond to the coumarin fluorophore and the molecular rotor respectively. The emission spectra of the rotor motif, when directly excited, are shown in Figure 2b, 2e and 2h for dyes **12**, **16** and **24** respectively. Figure 2c, 2f and 2i represent the viscosity sensitivity profiles of the ratiometric dyes.

Table 1 summarizes the spectroscopic data for all new compounds including, for comparison, those of compound **1**. Methoxycoumarin (donor) was exited near 355 nm and emitted at around 400 nm. The molecular rotor unit, either when excited through RET or excited directly, emits at around 490 nm for the thiophene rotors **12** and **24** and at around 485 nm for the aniline rotor **16** which is in accordance to previously reported data.

Since the equation (2) is logarithmic, data points of intensity versus viscosity in a double logarithmic plot would lie on a straight line. Extrapolation of this line for log(viscosity)=0 (i.e., the y-intercept) would then give the intensity of the dye in photon counts per second at a theoretical viscosity of 1 mPa•sec. It therefore gives information about the relative brightness of the dye, and it also combines the proportionality constants G, C, I_{EX} and c from equation (2).[18a,19] The term viscosity sensitivity refers to the exponent x in equations (1) and (3) and shows how much the rotor intensity increases as the viscosity increases. The exponent x can be obtained from the slop of the regression line in the double logarithmic plot. Moreover, the ratiometric intensity, shown in Table 1 (column 12), represents the ratio of rotor intensity over the donor intensity extrapolated at a theoretical viscosity of 1 mPa•sec. Qualitatively, this indicates how efficient is the RET between the primary and the secondary fluorophore.

In all cases the fluorescence of the coumarin donor was viscosity-independent. This can be evidenced by (a) the almost identical maximum intensity of the donor; and (b) the power law slope of the donor that remains almost zero. Small variations in the emission intensity, especially for compound **16** (Figure 2a), may be due to its limited solubility in higher viscosity solutions. Furthermore, upon direct excitation of the rotor, the y-intercept was higher than when excited through RET (Figure 2a/b, d/e and g/h). The lower rotor emission intensity through RET can be explained by the losses in the donor and by the donor emission itself, which both take away from the resonant energy that arrives at the donor. These findings are in accordance with previously reported data.[21c]

Comparison of hydrophilic dyes **12** and **16**, containing a thiophene- and an aniline-rotor respectively, indicates that **12** is brighter than **16** when excited directly (see Table 1, column 11). This is due to the **π**-system of **12** that is more electronically rich than that of **16**.[19] However, upon RET excitation, the brightness (y-intercept) of **16** is slightly higher than that of **12** (see Table 1, column 9). This can be explained by considering the more efficient excitation of the aniline fluorophore from the coumarin. Specifically, for **12** the λ_{max} of the coumarin emission is 404 nm while the λ_{max} for the thiophene excitation is 470 nm. On the other hand, in **16** the excitation maximum for the aniline dye is 436 nm allowing a more efficient RET. In the case of dye **16**, a better ratiometric intensity is also observed (see Table 1, column 12). Finally, the aniline-based rotor **16**, is more viscosity sensitive than the thiophene rotor **12** both when excited through RET or directly.

Comparison of the thiophene-based dyes **12**, **24** and **1** shows that they have almost the same sensitivity when excited through RET (Table 1, column 8). The above observation suggests that alterations of the linker between the two fluorophores and/or the substitution of the nitrogen donor do not affect the viscosity sensitivity of the dyes. In turn, this observation allows optimization of the physical properties of the probes, such as solubility and hydrophilicity, for a selected application. In all cases, whether the dyes are excited through RET or directly at the rotor, compound **24** shows higher brightness than **12** and **1**. This can be explained due to the size of the nitrogen substituens that block the rotation of the N-C bond and enhance the deexcitation through fluorescence. This event is pronounced in more viscous environments.[19]

2.5. Localization of self-calibrating dyes in cells

As illustrated in Figures 3 and 4, both compounds **12** and **24** can cross the cell membrane, but their localization pattern is distinctly different. The more hydrophilic compound **12** shows a relatively homogeneous distribution across the cell and absence of local concentrations that would be indicative of strong protein binding. Based on this, we conclude that **12** dissolves in the cytoplasm and remains in the aqueous phase. As such, **12** could serve as a self-calibrating dye suitable for viscosity measurements in the cytoplasm.

Conversely, **24** displays a non-uniform staining pattern in the cell. Analysis of emission intensity shows that **24** emits both from the cell membrane and from compartments inside the cell, most likely the cytoskeleton. Co-localization with the known membrane dye 1,1′-dioctadecyl-3,3,3′,3′-tetramethylindo carbocyanine (DiI) shows elevated fluorescence of **24** at locations preferred by DiI, that is, the cell membrane, but **24** exhibits even higher fluorescence from compartments inside the cell. It is known that a molecular rotor increases its fluorescence when it binds to a protein.[29] This behavior can explain the relatively high emission intensity from compartments inside the cell compared to emission from the cell membrane. Due to its relatively low localization specificity, **24** needs to be used in conjunction with a confocal microscope when it is intended as a membrane viscosity probe. Inside the cell, it can be used to study protein conformation, although the exact target proteins are subjects for further studies. The advantage of the ratiometric dye **24** compared to pure intensity-based studies with DCVJ[29] is that a calibration of the ratiometric intensity can provide the apparent viscosity of the microenvironment in mPa•sec.[23]

3. Conclusions

We present here the design, synthesis and spectroscopic evaluation of representative self-calibrating dyes. These dyes have been synthesized by covalently linking a coumarin (reference fluorophore) with a molecular rotor (viscosity sensor). Modifications on the linker between the molecular rotor and the coumarin do not affect significantly the fluorescence profile of these dyes. This can be further explored for optimization of

ratiometric viscosity probes toward specific applications. Subcellular localization studies of the new dyes show that they can cross the cell membrane and stay in the cytosol. Interestingly, hydrophilic dye **12** shows a homogeneous distribution inside the cell and represents a suitable probe for viscosity measurements in the cytoplasm. On the other hand, hydrophobic dye **24** behaves to some extent as a membrane dye, although it also crosses the cell membrane and likely binds to intracellular proteins, from where additional fluorescence is seen. Optimization of the chemical motif and fluorescence properties of self-calibrating dyes could provide probes for both microviscosity and bulk viscosity measurements.

4. Experimental

4.1. Chemistry

General notes—All reagents were purchased at highest commercial quality and used without further purification except where noted. Air- and moisture-sensitive liquids and solutions were transferred via syringe or stainless steel cannula. Organic solutions were concentrated by rotary evaporation below 40 °C at approximately 20 mmHg. All nonaqueous reactions were carried out under anhydrous conditions. Yields refer to chromatographically and spectroscopically (^{1}H NMR, ^{13}C NMR) homogeneous materials, unless otherwise stated. Reactions were monitored by thin-layer chromatography (TLC) carried out on 0.25 EMD TLC glass silica gel 60 F254 plates and visualized under UV light and/or developed by dipping in solutions of 10% ethanolic phosphomolybdic acid (PMA) and applying heat. Dynamic Adsorbents, Inc. silica gel (60, particle size 0.040–0.063 mm) was used for flash chromatography. NMR spectra were recorded on a Varian Mercury 400 MHz instrument and calibrated using the residual non-deuterated solvent as an internal reference. The following abbreviations were used to explain the multiplicities: s = singlet, d = doublet, t = triplet, m = multiplet, b = broad. High resolution mass spectra (HRMS) were recorded on a VG 7070 HS mass spectrometer under electron spray ionization (ESI) or electron impact (EI) conditions.

2-[2-(2-azidoethoxy)ethoxy]ethanol (3)—To a solution of 2-[2-(2-chloroethoxy)ethoxy]ethanol (**2**) (2 g, 11.86 mmol) in anhydrous DMF (18 ml), sodium azide (0.77 g, 11.86 mmol) potassium carbonate (14.3 g, 103 mmol) were added and stirred overnight at 90 °C. The mixture was cooled, diluted with THF (20 mL) and after stirring for 1 hour, it was filtered. The solid was washed with THF and the filtrate and washings were combined and concentrated to afford azide **3** (1.70 g, 82%). Crude compound **3** was used to the next step without further purification. ^{1}H NMR (400 MHz, $CDCl_3$) δ 3.75-3.72 (m, 2H), 3.69-3.66 (m, 6H), 3.62-3.60 (m, 2H), 3.39 (m, 2H); ^{13}C NMR (100 MHz, $CDCl_3$) δ 72.3, 70.2, 70.0, 69.6, 61.1, 50.3; HRMS calc for $C_6H_{13}N_3O_3Na$ $(M+Na)^+$ 198.0849 found 198.0848.

2-[2-(2-aminoethoxy)ethoxy]ethanol (4)—The above synthesized azide **3** (1.27 g, 7.25 mmol) was dissolved in MeOH (15 mL). Pd/C (0.22 g, 0.03 mmol) was added, the flask was purged of argon and filled with hydrogen. The solution was stirred overnight at room temperature. The mixture was filtered through celite and the solvent was evaporated to yield the pure amino alcohol **4** (1.03 g, 95%). **4:** light yellow oil; ^{1}H NMR (400 MHz, $CDCl_3$) δ 3.73-3.58 (m, 10H), 2.95 (bs, 2H), 2.82-2.79 (m, 2H); ^{13}C NMR (100 MHz, $CDCl_3$) δ 72.9, 70.4, 70.3, 61.7, 49.2; HRMS calc for $C_6H_{16}NO_3$ $(M+H)^+$ 150.1125 found 150.1125.

tert-butyl N-{2-[2-(2-hydroxyethoxy)ethoxy]ethyl} carbamate (5)—Di-tert-butyl dicarbonate (1.75 g, 8.04 mmol) was added to a solution of amino alcohol **4** (600 mg, 4.02 mmol) in a 9:1 (v/v) mixture of methanol/triethylamine (68 ml). The reaction was left stirring under reflux and upon completion, the solvent was removed under reduced pressure

and the residue extracted with DCM/water. The organic layer was dried over anhydrous $MgSO_4$ and concentrated under reduced pressure to yield **5** (902 mg, 90%). **5:** yellow oil; ^{1}H NMR (400 MHz, $CDCl_3$) δ 3.77-371 (m, 2H), 3.66-3.55 (m, 8H), 3.49-3.31 (m, 2H), 1.45 (s, 9H); ^{13}C NMR (100 MHz, $CDCl_3$) δ 156.2, 79.9, 73.0, 70.6, 70.5, 70.0, 61.9, 40.5, 28.6; HRMS calc for $C_{11}H_{24}NO_5$ $(M+H)^+$ 250.1654 found 150.1649.

β-cyanoacetate 7—To a round bottom flask containing a solution of the BOC-protected amino alcohol **5** (750 mg, 3.01 mmol) and cyanoacetic acid (260 mg, 3.01 mmol) in 6 mL of anhydrous DCM, EDC (470 mg, 3.02 mmol) and HOBT (408 mg, 3.02 mmol) were added. The formation of the product was monitored by TLC and was completed after overnight stirring at room temperature. The crude mixture was concentrated under reduced pressure and the product was purified via flash chromatography (50–70% EtOAc-hexanes). **7** (743 mg, 78% yield) as light yellow oil; ^{1}H NMR (400 MHz, $CDCl_3$) δ 5.00 (bs, 1H), 4.37 (m, 2H), 3.74 (m, 2H), 3.64 (m, 4H), 3.53 (m, 4H), 3.31 (s, 2H), 1.44 (s, 9H); ^{13}C NMR (100 MHz, $CDCl_3$) δ 163.2, 156.3, 113.1, 79.8, 70.8, 70.5, 70.4, 68.7, 66.0, 40.5, 28.6, 24.9; HRMS calc for $C_{14}H_{24}N_2O_6Na$ $(M+Na)^+$ 339.1527 found 339.1525.

Carbamate 9—To a round bottom flask, compounds **7** (200 mg, 0.63 mmol) and **8** (122 mg, 0.63 mmol) were dissolved in dry THF (5 mL). To that, DBU (0.01 mL, 0.06 mmol) was added and left stirring at room temperature. Upon completion, the crude solution was concentrated under reduced pressure and purified via flash chromatography (30–50% EtOAchexanes) to yield **9** (193 mg, 62% yield) as yellow solid. ^{1}H NMR (400 MHz, $CDCl_3$) δ 8.00 (s, 1H), 7.41 (bs, 1H), 6.08 (d, 1H, J = 4.6 Hz), 5.10 (bs, 1H), 4.35 (m, 2H), 3.76 (m, 2H), 3.67 (m, 2H), 3.60 (m, 2H), 3.52 (m, 2H), 3.42 (m, 4H), 3.29 (m, 2H), 1.67 (m, 6H), 1.40 (s, 9H); ^{13}C NMR (100 MHz, $CDCl_3$) δ 169.7, 165.3, 156.3, 146.7, 144.4, 120.0, 118.7, 105.2, 79.3, 70.9, 70.5, 70.5, 69.3, 64.7, 51.5, 40.6, 29.9, 28.6, 25.3, 23.7; HRMS calc for $C_{24}H_{36}N_3O_6S$ $(M+H)^+$ 494.2319 found 494.2316.

Ratiometric dye 12—A TFA solution was prepared by combining 5 mL of TFA with 0.1 mL of anisole in 4.9 mL of DCM. 0.90 mL of this solution was added to **9** (45 mg, 0.09 mmol) and the reaction was left stirring at room temperature. After 30 minutes, reaction was completed and the solution was concentrated, rinsed with toluene (4 × 10 ml), concentrated, and dried under high vacuum to yield **10**, which was used immediately to the next step. To a round bottom flask containing **10** dissolved in dry DCM (0.6 mL); DMAP (1 mg, 0.009 mmol), *N*-succinimidyl-7-methoxycoumarin-3- carboxylate (**11**) (27 mg, 0.08 mmol), and DIPEA (0.03 mL, 0.17 mmol) were added. The reaction was left stirring at room temperature and monitored by TLC. Upon completion, the reaction was concentrated under reduced pressure and purified via flash chromatography (30–50% EtOAc-hexanes) to yield **12** (44 mg, 83% yield) as orange solid. ^{1}H NMR (400 MHz, $CDCl_3$) δ 9.05 (bs, 1H), 8.79 (s, 1H), 7.97 (s, 1H), 7.56 (d, 1H, J = 8.7 Hz), 7.39 (bs, 1H), 6.89 (dd, 1H, J = 2.1 Hz, J = 8.7 Hz), 6.81 (d, 1H, J = 2.1 Hz), 6.06 (d, 1H, J = 4.6 Hz), 4.36 (m, 2H), 3.88 (s, 3H), 3.79 (m, 2H), 3.72-3.63 (m, 8H), 3.41 (m, 4H), 1.67 (bs, 6H); ^{13}C NMR (100 MHz, $CDCl_3$) δ 172.3, 169.6, 165.3, 165.0, 162.6, 161.7, 156.8, 148.4, 146.5, 144.2, 131.1, 119.9, 118.5, 114.7, 114.1, 112.5, 105.0, 100.4, 70.9, 70.7, 69.7, 69.3, 64.7, 63.9, 56.2, 51.4, 36.9, 25.2, 23.6; HRMS calc for $C_{30}H_{34}N_3O_8S$ $(M+H)^+$ 596.2061 found 596.2060.

Carbamate 14—To a solution of commercially available compound **13** (94 mg, 0.63 mmol) and **7** (200 mg, 0.63 mmol) in dry THF (2.4 mL), DBU (0.01 mL, 0.06 mmol) was added and left stirring at room temperature. Upon completion, the solution was concentrated under reduced pressure and the product was purified via flash chromatography (30–50% EtOAc-hexanes) to yield **14** (189 mg, 67% yield) as yellow solid. ^{1}H NMR (400 MHz, $CDCl_3$) δ 8.08 (s, 1H), 7.94 (d, 2H, J = 9.1 Hz), 6.70 (d, 2H, J = 9.1 Hz), 5.05 (bs, 1H), 4.43

(m, 2H), 3.81 (m, 2H), 3.71 (m, 2H), 3.63 (m, 2H), 3.55 (m, 2H), 3.32 (m, 2H), 3.12 (s, 6H), 1.43 (s, 9H); ^{13}C NMR (100 MHz, $CDCl_3$) δ 164.5, 156.2, 155.0, 153.9, 134.4, 119.5, 117.6, 111.7, 93.7, 79.3, 71.0, 70.5, 70.5, 69.1, 65.2, 40.6, 40.2, 28.6; HRMS calc for $C_{23}H_{34}N_3O_6$ $(M+H)^+$ 448.2442 found 448.2439.

Ratiometric dye 16—A TFA solution was prepared by combining 5 mL of TFA with 0.1 mL of anisole in 4.9 mL of DCM. 1.1 mL of this solution was added to **14** (50 mg, 0.11 mmol) and the reaction was left stirring at room temperature. After 30 minutes, reaction was completed and the solution was concentrated, rinsed with toluene (4 × 10 ml), concentrated again, and dried under high vacuum to yield compound **15**. To a round bottom flask containing **15** in dry DCM (0.8 mL); DMAP (1 mg, 0.01 mmol), *N*-succinimidyl-7-methoxycoumarin-3-carboxylate (**11**) (34 mg, 0.10 mmol), and DIPEA (0.04 mL, 0.22 mmol) were added. The reaction was left stirring overnight at room temperature. Upon completion, the reaction was concentrated and purified via flash chromatography (30–50% EtOAc: hexanes) to yield ratiometric dye **16** (49 mg, 81% yield) as orange solid. ^{1}H NMR (400 MHz, $CDCl_3$) δ 9.06 (bs, 1H), 8.81 (s, 1H), 8.04 (s, 1H), 7.89 (d, 2H, J = 9.0 Hz), 7.56 (d, 1H, J = 8.7 Hz), 6.90 (dd, 1H, J = 2.2 Hz, J = 8.7 Hz), 6.82 (d, 1H, J = 2.2 Hz), 6.66 (d, 2H, J = 9.0 Hz), 4.43 (m, 2H), 3.89 (s, 3H), 3.84 (m, 2H), 3.74 (m, 2H), 3.70-3.65 (m, 6H), 3.09 (s, 6H); ^{13}C NMR (100 MHz, $CDCl_3$) δ 165.0, 164.5, 162.6, 161.8, 156.9, 154.9, 153.8, 148.5, 134.3, 131.1, 119.5, 117.6, 114.9, 114.2, 112.6, 111.7, 100.4, 93.9, 71.0, 70.8, 69.8, 69.2, 65.3, 56.2, 40.2, 39.9; HRMS calc for $C_{29}H_{31}N_3O_8Na$ $(M+Na)^+$ 572.2003 found 572.2005.

5-(dihexylamino)thiophene-2-carbaldehyde (18)—2-bromo- 5-formylthiophene (**17**) (0.4 g, 2.09 mmol), dihexylamine (1.5 mL, 6.28 mmol) and *p*-toluenesulfonic acid (20 mg, 0.06 mmol) were heated at 100 °C for 24 hours. The mixture was cooled and 5 mL of water were added. After stirring for an additional half hour, the product was extracted with CH_2Cl_2. The solution was dried over $MgSO_4$, concentrated under reduced pressure and purified via flash chromatography (5–50% EtOAc:hexanes) to yield **18** (518 mg, 83% yield) as oil. ^{1}H NMR (400 MHz, $CDCl_3$) δ 9.38 (d, 1H, J = 1.0 Hz), 7.37 (d, 1H, J = 4.3 Hz), 5.83 (dd, 1H, J = 1.0 Hz, J = 4.3 Hz), 3.25 (m, 4H), 1.58 (m, 4H), 1.24 (bs, 12H), 0.83 (m, 6H); ^{13}C NMR (100 MHz, $CDCl_3$) δ 179.5, 167.0, 140.7, 125.1, 102.7, 53.8, 31.5, 26.5, 22.6, 14.0; HRMS calc for $C_{13}H_{22}N_2O_4Na$ $(M+Na)^+$ 293.1472 found 293.1473.

Carbamate 22—To a solution of compound **18** (130 mg, 0.44 mmol) and **21**[21c] (100 mg, 0.37 mmol) in dry THF (2.9 mL), DBU (0.08 mL, 0.53 mmol) was added and left stirring at room temperature. Upon completion, the solution was concentrated under reduced pressure and the product was purified via flash chromatography (10–30% EtOAc-hexanes) to yield **22** (169 mg, 70% yield) as orange solid. ^{1}H NMR (400 MHz, $CDCl_3$) δ 7.96 (bs, 1H), 7.35 (bs, 1H), 5.95 (d, 2H, J = 4.4 Hz), 4.61 (bs, 1H), 4.18 (t, 2H, J = 6.6 Hz), 3.35 (m, 4H), 3.09 (m, 2H), 1.73-1.57 (m, 6H), 1.54-1.47 (m, 2H), 1.41 (bs, 11H), 1.28 (m, 12H), 0.87 (m, 6H); ^{13}C NMR (100 MHz, $CDCl_3$) δ 168.6, 165.6, 156.1, 146.1, 144.6, 119.3, 118.8, 104.4, 79.1, 65.2, 54.0, 40.5, 31.6, 29.8, 28.5, 27.1, 26.6, 23.4, 22.7, 14.1; HRMS calc for $C_{30}H_{50}N_3O_4S$ $(M+H)^+$ 570.3336 found 570.3333.

Ratiometric dye 24—A TFA solution was prepared by combining 5 mL of TFA with 0.1 mL of anisole in 4.9 mL of DCM. 1.1 mL of this solution was added to **22** (60 mg, 0.11 mmol) and the reaction was left stirring at room temperature. After 30 minutes, reaction was completed and the solution was concentrated, rinsed with toluene (4 × 10 ml), concentrated again, and dried under high vacuum to yield compound **23**. To a round bottom flask containing **23** in dry DCM (2.0 mL); DMAP (1 mg, 0.01 mmol), *N*-succinimidyl-7-methoxycoumarin-3-carboxylate (**11**) (38 mg, 0.12 mmol), and DIPEA (0.04 mL, 0.25

mmol) were added. The reaction was left stirring overnight at room temperature. Upon completion, the reaction was concentrated and purified via flash chromatography (10–30% EtOAc: hexanes) to yield ratiometric dye **24** (60 mg, 84% yield) as orange solid. ^{1}H NMR (400 MHz, $CDCl_3$) δ 8.83 (s, 1H), 8.78 (s, 1H), 7.99 (bs, 1H), 7.57 (d, 2H, J = 8.7 Hz), 7.40 (bs, 1H), 6.93 (dd, 1H, J = 2.4 Hz, J = 8.7 Hz), 6.86 (d, 1H, J = 2.3 Hz), 5.96 (d, 1H, J = 4.6 Hz), 4.23 (t, 2H, J = 6.7 Hz), 3.91 (s, 3H), 3.47 (m, 2H), 3.37 (m, 4H), 1.81-1.74 (m, 2H), 1.70-1.62 (m, 8H), 1.54-1.46 (m, 2H), 1.35-1.27 (m, 12H), 0.86 (m, 6H); ^{13}C NMR (100 MHz, $CDCl_3$) δ 168.6, 165.7, 164.9, 162.2, 162.1, 156.8, 148.4, 146.2, 144.6, 131.1, 119.4, 118.8, 115.1, 114.1, 112.7, 104.4, 100.5,65.2, 56.2, 54.1, 39.8, 31.7, 29.9, 29.4, 28.7, 27.2, 26.7, 23.6, 22.8, 14.2; HRMS calc for $C_{36}H_{47}N_3O_6SNa$ $(M+Na)^+$ 672.3078 found 672.3082.

4.2. General procedure for the determination of spectral properties

Each viscosity sample was mixed according to the volumes shown in the first column in Table 2 below. Viscosity of each sample was estimated by the summation of weighted ratio[30] of each solvent's viscosity at 25 °C from the 92st Edition of the CRC Handbook of Chemistry and Physics, 2011–2012. The glycerol (Gly) was heated to ensure more exact measuring during pipetting. The pre-stained ethylene glycol (EG) for each sample contained 100 μM of dye resulting in a final concentration of 10 μM for each sample. All samples were placed on rotating mixer for a minimum of 1 hour before pouring into cuvettes for scanning. Preliminary fluorescent scanning was done on each dye dissolved in 414.4 mPa•sec viscosity solvent to determine optimal excitation and peak emission and slit settings for each molecular rotor derivative. All fluorescent scanning was done in a Fluoromax-3 photoncounting spectrophotometer (Jobin-Yvon) with the temperature-controlled turret (Quantum Northwest) set at room temperature (22 °C). Each sample was inserted in the turret and allowed to equilibrate for 10 minutes before testing. The monochromator slit settings for all calculations were 5 nm. For each solvent the fluorescent emission in an 11 nm range around peak emission was averaged and the logarithm of the average peak intensity was plotted against the logarithm of the viscosity. The slope was obtained for each molecular rotor derivative by linear regression (Graphpad Prism 4.01, San Diego, CA). The exponent *x* of each viscosity gradient was used to evaluate viscosity sensitivity, with a higher value of the exponent *x* indicating higher sensitivity. R^2 values indicate the linear regression of the log-transformed data (intensity over viscosity).

4.3. General procedure for cell culture staining and imaging

Immortalized T24 human bladder epithelial cells (HTB-4™ ATCC, Manassas VA USA) were grown to confluence on glass culture slides (Fisher Scientific, Pittsburg PA USA). The cells were pre-stained with an aqueous Vybrant DiI (Invintrogen) solution as suggested by Invitrogen/Molecular Probes.[31] A liposome solution was prepared. 200μl of 1,2-dilauroyl-sn-glycero-phosphocholine (Avanti Polar Lipids, Inc., Alabaster AL USA) in chloroform and 200μl of chloroform (Sigma-Aldrich St Louis MO USA) were added to a small glass vial. 50μl of 5mM dye solution in chloroform was added. Chloroform was evaporated while phial was rotated creating a thin layer on the inner walls of the vial. 1ml of Ca^{2+} and Mg^{2+} free phosphate buffered Saline (PBS, Sigma- Aldrich St Louis MO USA) solution was added. The solution is treated to 3 cycles of 10 minutes in a water bath at 37°C and 5 minutes in an ice bath. The solution was then extruded 11 times through a 0.1μm membrane with the Avanti Mini- Extruder creating 0.1μm liposomes. Liposome solution was added to serum-free McCoy's 5A modified media (Sigma Aldrich, St. Louis MO USA) at a ratio of 1:9. A 500μl volume of liposome-media solution is added to the slide wells and allowed to incubate for 30 minutes at 37°C and 5% CO_2. The dye concentration applied to the cells during staining is estimated at 25μM by dilution. Staining solution was removed and the slides gently washed with serum-free PBS. Images were taken at 60X magnification using Olympus IX71 microscope with both WBV (exciter D425/40X, emitter 475lpv2,

beamsplitter 450dcxr) and TRITC (exciter D540/25X emitter D605/55m beamsplitter 565dclp) cube filters with an Apogee Alta 2000 camera. A composite image was created from the WBV image (green channel) and the corresponding TRITC image (red channel) and the image was reduced in size by binning a 2×2 pixel area. Image processing and extraction of the intensity profiles were performed with Crystal Image.[32]

A 20mM stock solution of compound **12** in DMSO was prepared and it was then diluted and used at a final concentration of 2μM in DMEM medium. HeLa cells were maintained at 37 °C in a 5% CO_2 incubator in DMEM supplemented with 10% FBS. The day prior to the experiment the cells were plated on 35mm Ibidi dishes (Biovalley #81156) at 70% confluency. The probes were added at 2μM concentration into DMEM. Control cells were treated with DMSO at 0.1%. After 1h incubation, the cells were washed three times with DMEM and then kept into DMEM supplemented with 25mM HEPES (pH=7.4). The cells were then imaged live using a Zeiss Observer Z1 156 inverted microscope with 63× objective controlled by AxioVision software (Zeiss, Thornwood, NY).

Supplementary Material

Refer to Web version on PubMed Central for supplementary material.

Acknowledgments

Financial support from the National Institutes of Health (1R21 RR025358 and CA 133002) is gratefully acknowledged. We thank the NSF for instrumentation grants CHE-9709183 and CHE-0741968. We also thank Drs. A. Mrse and Dr. Y. Su for NMR and MS assistance respectively.

References and notes

1. Shinitzky, M. Physiology of membrane fluidity. Shinitzky, M., editor. Vol. 1. CRC Press; Boca Raton, FL: 1984. p. 1-51.
2. (a) Luby-Phelps K. Int Rev Cytol. 2000; 192:189–221. [PubMed: 10553280] (b) Molecular and Cellular Aspects of Basement Membranes. Academic; San Diego, CA: 1993. (c) The Membranes of Cells. Academic; San Diego, CA: 1993. (d) Membrane Abnormalities in Sickle Cell Disease and in other Red Blood Cell Disorders. CRC; Boca Raton, FL: 1994.
3. (a) Reinhart WH. Biorheology. 2001; 38:203–212. [PubMed: 11381175] (b) Moriarty PM, Gibson CA. Cardiovasc Rev Rep. 2003; 24:321–325.(c) Uchimura I, Numano F. Diabetes Frontier. 1997; 8:33–37.(d) Simon A, Gariepy J, Chironi G, Megnien JL, Levenson JJ. J Hypertens. 2002; 20:159–169. [PubMed: 11821696]
4. Luneva OG, Brazhe NA, Maksimova NV, Rodnenkov OV, Parsina EY, Bryzgalova NY, Maksimov GV, Rubin AB, Orlov SN, Chazov EI. Pathophysiology. 2007; 14:41–46. [PubMed: 17403600]
5. (a) Goodwin JS, Drake KR, Remment CL, Kenworthy AK. Biophys J. 2005; 89:1398–1410. [PubMed: 15923235] (b) Dibner MD, Ireland KA, Koerner LA, Dexter DL. Cancer Res. 1985; 45:4998–5003. [PubMed: 4027982]
6. (a) Aleardi AM, Benard G, Augereau O, Malgat M, Talbot JC, Mazat JP, Letellier T, Dachary-Prigent J, Solaini GC, Rossignol R. J Bioenerg Biomembr. 2005; 37:207–225. [PubMed: 16167177] (b) Hou X, Richardson SJ, Aguilar MI, Small DH. Biochemistry. 2005; 44:11618–11627. [PubMed: 16114899]
7. (a) Ahn JH, Kim TY, Kim YJ, Han MW, Yoon TH, Chung JW. Diabetic Med. 2006; 23:1339–1343. [PubMed: 17116185] (b) Salazar Vazquez BY, Salazar Vasquez MA, Venzor VC, Negrete AC, Cabrales P, Diaz JS, Intaglietta M. Clin Hemorheol Microcirc. 2008; 38:67–74.
8. Kearney-Schwartz A, Virion J-M, Stoltz J-F, Drouin P, Zannad F. Fundam Clin Pharmacol. 2007; 21:387–396. [PubMed: 17635177]
9. Bosman GJCGM, Bartholomeus IGP, de Grip WJ. Gerontology. 1991; 37:95–112. [PubMed: 1647364]

10. (a) Möller W, Takenaka S, Rust M, Stahlhofen W, Heyer J. J Aerosol Med. 1997; 10:173–186. [PubMed: 10174196] (b) Butler JP, Kelly SM. Biorheology. 1998; 35:193–209. [PubMed: 10474651] (c) Valberg PA, Albertini DF. J Cell Biol. 1985; 101:130–140. [PubMed: 4040136]
11. (a) International Committee for Standardization in Haematology. J Clin Pathol. 1984; 37:1147–1152. [PubMed: 6490952] (b) Wang S, Boss AH, Kensey KR, Rosenson RS. Clin Chim Acta. 2003; 332:79–82. [PubMed: 12763283]
12. Lakowicz, JR. Principles of Fluorescence Spectroscopy. Springer; New York, NY: 2006.
13. (a) Kuimova MK, Yahioglu G, Levitt JA, Suhling K. J Am Chem Soc. 2008; 130:6672–6673. [PubMed: 18457396] (b) Kuimova MK, Botchway SW, Parker AW, Balaz M, Collins HA, Anderson HL, Suhling K, Ogilby PR. Nat Chemistry. 2009; 1:69–73.(c) Peng X, Yang Z, Wang J, Fan J, He Y, Song F, Wang B, Sun S, Qu J, Qi J, Yan M. J Am Chem Soc. 2011; 133:6626–6635. [PubMed: 21476543]
14. Shinitzky M, Barenholz Y. Biochim Biophys Acta. 1978; 515:367–394. [PubMed: 365237]
15. (a) Axelrod D, Koppel DE, Schlessinger J, Elson E, Webb WW. Biophys J. 1976; 16:1055–1069. [PubMed: 786399] (b) Soumpasis DM. Biophys J. 1983; 41:95–97. [PubMed: 6824758] (c) Swaminathan R, Bicknese S, Periasamy N, Verkman AS. Biophys J. 1996; 71:1140–1151. [PubMed: 8842251]
16. Blonk JCG, Don A, van Aalst H, Birmingham JJ. J Microsc. 1993; 169:363–374.
17. For selected recent reviews on this topic see: Haidekker MA, Theodorakis EA. Org Biomol Chem. 2007; 5:1669–1678. [PubMed: 17520133] Demchenko P, Mely Y, Duportail G, Klymchenko AS. Biophys J. 2009; 96:3461–3470. [PubMed: 19413953] Haidekker MA, Nipper ME, Mustafic A, Lichlyter D, Dakanali M, Theodorakis EA. Demchenko AP. In Advanced Fluorescence Reporters in Chemistry and Biology I. Fundamentals, and Molecular Design. Springer-Verlag2010:267–308.
18. (a) Haidekker MA, Theodorakis EA. J Biol Eng. 2010; 4:11. [PubMed: 20843326] (b) Grabowski ZR, Rotkiewicz K, Rettig W. Chem Rev. 2003; 103:3899–4031. [PubMed: 14531716]
19. Sutharsan J, Lichlyter D, Wright NE, Dakanali M, Haidekker MA, Theodorakis EA. Tetrahedron. 2010; 66:2582–2588. [PubMed: 20694175]
20. Förster T, Hoffmann Z. Phys Chem. 1971; 75:63–76.
21. (a) Haidekker MA, Brady TP, Lichlyter D, Theodorakis EA. J Am Chem Soc. 2006; 128:398–399. [PubMed: 16402812] (b) Fischer D, Theodorakis EA, Haidekker MA. Nat Protoc. 2007; 2:227–236. [PubMed: 17401358] (c) Yoon HJ, Dakanali M, Lichlyter D, Chang WM, Nguyen KA, Nipper ME, Haidekker MA, Theodorakis EA. Org Biomol Chem. 2011; 9:3530–3540. [PubMed: 21437318]
22. Förster T. Ann Phys. 1948; 437:55–75.
23. Nipper ME, Dakanali M, Theodorakis EA, Haidekker MA. Biochimie. 2011; 93:988–994. [PubMed: 21354253]
24. Tabatadze D, Zamacnik P, Yanachkov I, Wright G, Pierson K, Zhang S, Bogdanov A Jr, Metelev V. Nucleosides, Nucleotides and Nucleic Acids. 2008; 27:157–172.
25. Salvagnini C, Gharbi S, Boxus T, Marchand-Brynaert J. Eur J Med Chem. 2007; 42:37–53. [PubMed: 17010480]
26. Rerat V, Dive G, Cordi AA, Tucker GC, Bareille R, Amédée J, Bordenave L, Marchand-Brynaert J. J Med Chem. 2009; 52:7029–7043. [PubMed: 19860432]
27. Prim D, Kirsch G, Nicoud J-F. Synlett. 1998:383–384.
28. Yan P, Xie A, Wei M, Loew LM. J Org Chem. 2008; 73:6587–6594. [PubMed: 18665648]
29. (a) Iio T, Itakura M, Takahasi S, Sawada S. J Biochem. 1991; 109:499–502. [PubMed: 1869503] (b) Iio T, Takashi S, Sawada S. J Biochem. 1993; 113:196–199. [PubMed: 8468324] (c) Iwaki T, Torigoe C, Noji M, Nakanishi M. Biochemistry. 1993; 32:7589–7592. [PubMed: 8338855] (d) Kung CE, Reed JK. Biochemistry. 1986; 25:6114–6121.
30. Akers W, Haidekker MA. J Biomech Eng-Trans ASME. 2004; 126:340–345.
31. Molecular Probes product information for Vibrant cell-labeling solutions. http://probes.invitrogen.com/media/pis/mp22885.pdf
32. Haidekker, MA. Advanced biomedical image analysis. Haidekker, MA., editor. John Wiley & Sons; Hoboken, NJ: 2011. p. 441-474.

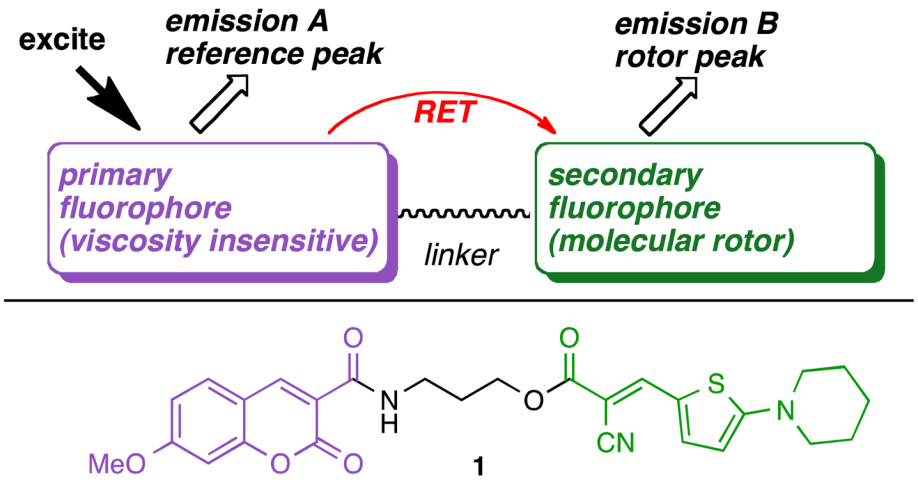

Figure 1.
General design of ratiometric self-calibrating viscosity sensors.

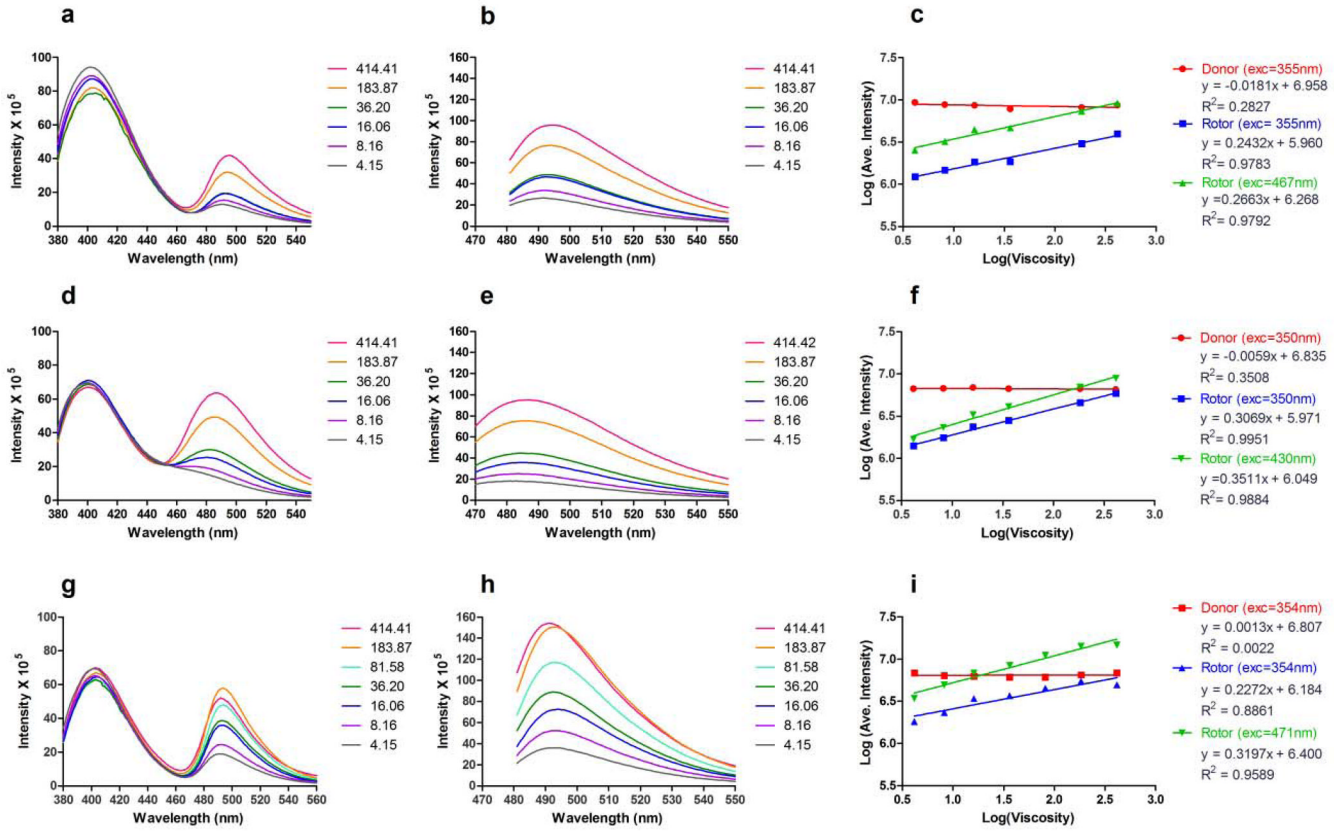

Figure 2.

Fluorescence emission spectra and viscosity sensitivity plots of hydrophilic ratiometric dyes **12** (Fig a, b, c), **16** (Fig. d, e, f) and **24** (Fig. g, h, i) in ethylene glycol:glycerol (or MeOH) mixtures (viscosity is recorded in mPa•sec). Fig. a, d, g: emission spectra via RET; Fig. b, e, h: emission spectra under direct excitation of the rotor motif; Fig. c, f, i: viscosity sensitivity plots.

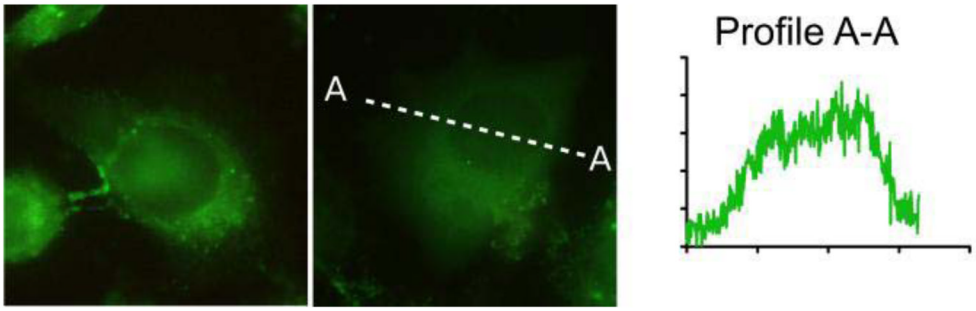

Figure 3.
Representative He-La cells stained with **12**. The dye exhibits a fairly homogeneous distribution inside the cell. The intensity profile along the dashed line A-A further illustrates the homogeneous dye distribution.

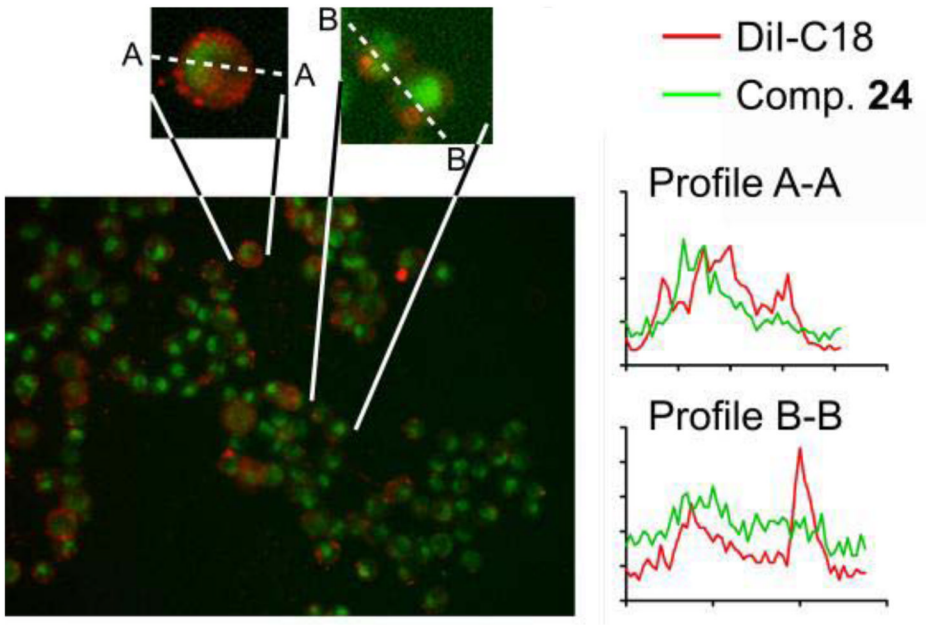

Figure 4.

Representative T-24 cells dual-labeled with **24** (green) and the membrane dye DiI-C18 (red). Dye **24** exhibits a more complex staining pattern with a clear preference for intracellular compartments. Magnified sections and the intensity profiles along the dashed lines A-A and B-B show that a moderate correlation between the locales of DiI and **24** exists.

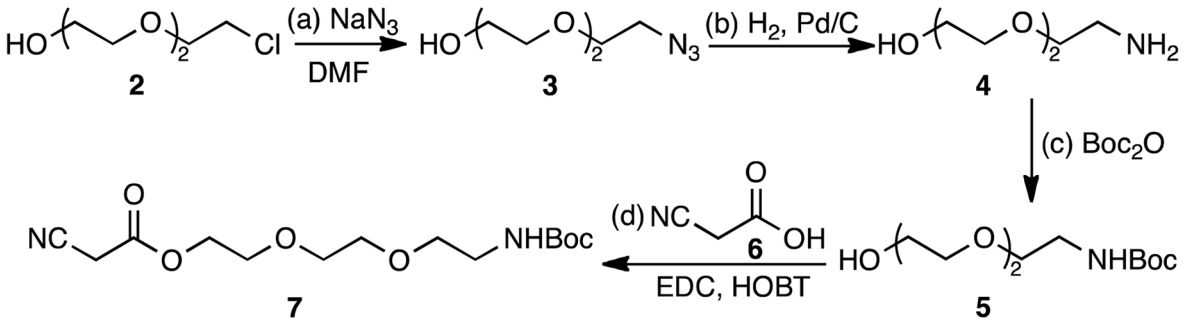

Scheme 1.

Reagents and conditions: (a) 1.0 equiv. **2**, 1.0 equiv. NaN_3, DMF, 18 h, 90 °C, 82%; (b) 0.05 equiv. Pd/C, methanol, 18 h, 25 °C, 95%; (c) 1.0 equiv. **4**, 2.0 equiv. Boc_2O, 2.0 equiv. Et_3N, methanol, 18 h, reflux, 90%; (d) 1.0 equiv. **5**, 1.0 equiv. **6**, 1.1 equiv. EDC, 1.1 equiv. HOBT, CH_2Cl_2, 18 h, 25 °C, 78%.

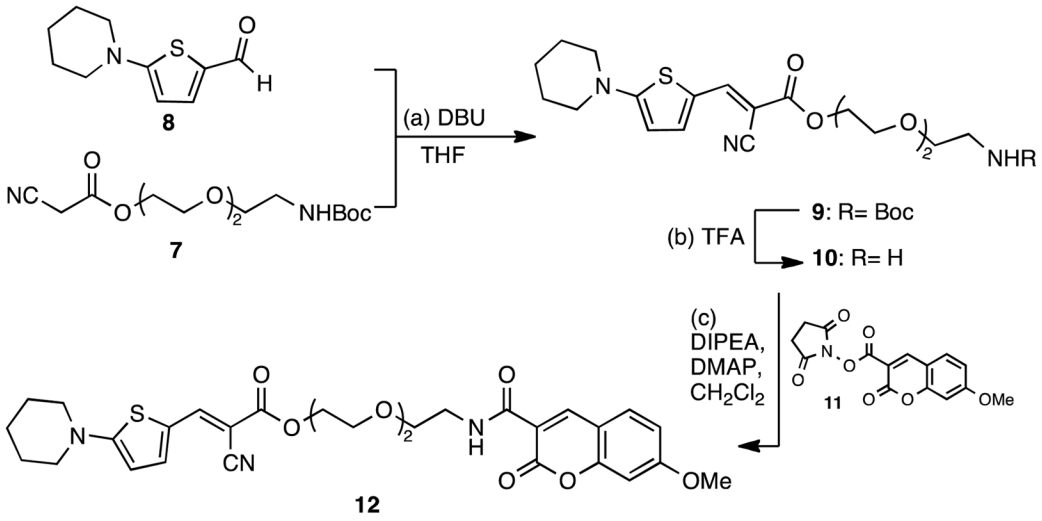

Scheme 2.

Reagents and conditions: (a) 1.0 equiv. **7**, 1.5 equiv. **8**, 0.1 equiv. DBU, 18 h, 25 °C, 62%; (b) 1.0 equiv. **9**, TFA/CH_2Cl_2, 30 min, 25 °C; (c) 1.0 equiv. **11**, 1.1 equiv. **10**, 2.0 equiv. DIPEA, 0.1 equiv. DMAP, CH_2Cl_2, 18 h, 25 °C, 83% (over two steps).

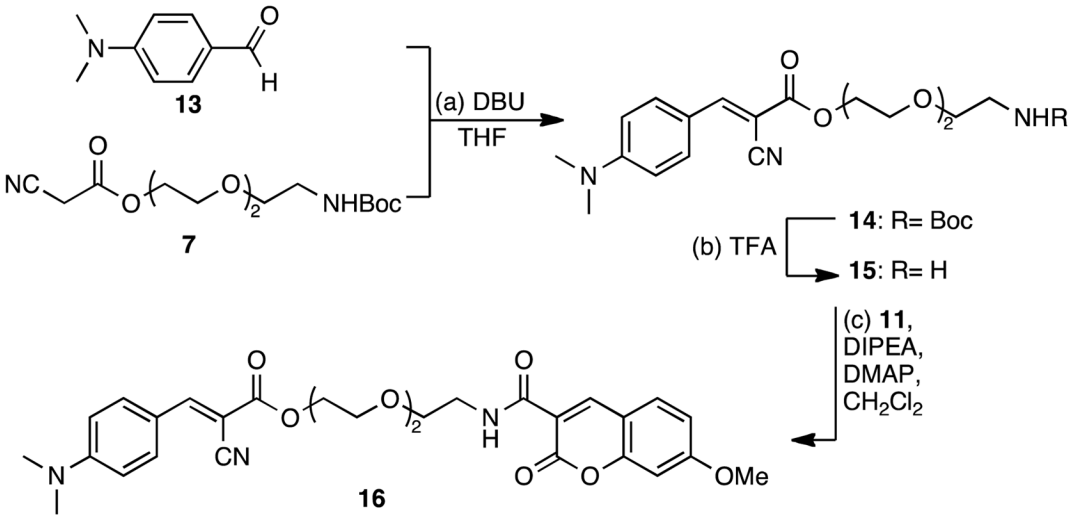

Scheme 3.

Reagents and conditions: (a) 1.0 equiv. **7**, 1.5 equiv. **13**, 0.1 equiv. DBU, 18 h, 25 °C, 67%; (b) 1.0 equiv. **14**, TFA/CH_2Cl_2, 30 min, 25 °C; (c) 1.0 equiv. **15**, 1.1 equiv. **11**, 2.0 equiv. DIPEA, 0.1 equiv. DMAP, CH_2Cl_2, 18 h, 25 °C, 81% (over two steps).

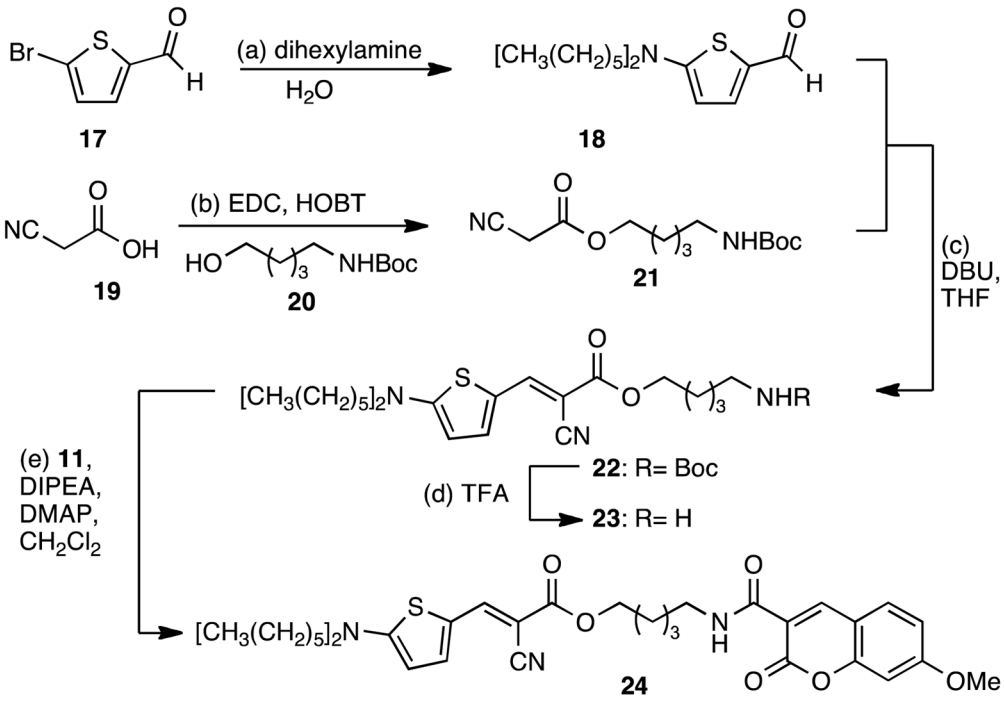

Scheme 4.

Reagents and conditions: (a) 1.0 equiv. **17**, 3.0 equiv. dihexylamine, H_2O, 18 h, 100 °C, 83%; (b) 1.0 equiv. **19**, 1.6 equiv. **20**, 1.1 equiv. EDC, 1.1 equiv. HOBT, CH_2Cl_2, 18 h, 25 °C, 73%; (c) 1.2 equiv. **18**, 1.0 equiv. **21**, 1.1 equiv. DBU, THF, 18 h, 25 °C, 70%; (d) 1.0 equiv. **22**, TFA/CH_2Cl_2, 30 min, 25 °C; (e) 1.0 equiv. **23**, 0.95 equiv. **11**, 2.0 equiv. DIPEA, 0.1 equiv. DMAP, CH_2Cl_2, 2 h, 25 °C, 84% (over two steps).

Table 1

Fluorescent properties and viscosity sensitivity of the dyes

	Donor				Rotor						Ratiometric intensity
Cmp	**Exc λ (nm)**	**Em λ (nm)**	**Power-law slope of donor**	**y-intercept (10^6 cps)**	**Exc λ (nm)**	**Em λ (nm)**	**Viscosity sensitivity (*donor exc*)**	**y-intercept (*donor exc*) ($\times 10^6$ cps)**	**Viscosity sensitivity (*rotor exc*)**	**y-intercept (*rotor exc*) ($\times 10^6$ cps)**	**I_{Em}/I_{ref} (*donor exc*)**
12	355	400	−0.018	9.08	467	492	0.24	0.91	0.23	1.86	0.10
16	350	400	−0.0059	6.84	430	485	0.31	0.94	0.35	1.12	0.14
24	354	401	0.0013	6.41	471	491	0.23	1.53	0.32	2.51	0.24
1	354	402	0.0055	6.86	467	494	0.23	0.81	0.24	1.98	0.12

Bioorg Med Chem. Author manuscript; available in PMC 2013 July 15.

Table 2

Solvent composition and viscosity

Pre-stained EG / EG / Gly or MeOH volumes (ml)	Viscosity (mPa •sec)	Log Viscosity
0.5 / 0.5 / 4.0	414.4	2.62
0.5 / 1.5 / 3.0	183.8	2.26
0.5 / 3.5 / 1.0	36.2	1.56
0.5 / 4.5 / 0.0	16.1	1.21
0.5 / 3.5 / 1.0 (MeOH)	8.16	0.91
0.5 / 2.5 / 2.0 (MeOH)	4.15	0.62